The International Journal of Advanced Manufacturing Technology (2018) 95:2835–2842
https://doi.org/10.1007/s00170-017-1407-6

ORIGINAL ARTICLE

Effects of electropulsing on the machinability and microstructure of GH4169 superalloy during turning process

Z. Sun [1,2] · H. Wang [1,2] · Y. Ye [1,2] · Z. Xu [1,2] · G. Tang [1]

Received: 10 July 2017 / Accepted: 13 November 2017 / Published online: 30 November 2017

Abstract
The effects of electropulsing on the machinability and microstructure of the machined surface of GH4169 superalloy are investigated in the present work. The results indicate that the machinability and the surface quality of GH4169 superalloy achieve evident improvements during the electropulsing-assisted turning process (EP-TP) at appropriate electropulsing parameters compared with the traditional dry turning process (TD-TP). In EP-TP at the frequency of 400 Hz and the root-mean-square (RMS) current density of 0.64 A mm^{-2}, the main cutting force, the axial surface roughness, and the surface microhardness are reduced dramatically. In addition, the quality of machined surface and the ability of plastic deformation are also facilitated significantly under the effects of electropulsing. For GH4169 superalloy, the enhanced ability of the plastic deformation and the promoted mobility of dislocations in the cutting layer under the influence of the coupling of thermal and athermal effects of the exerted electropulsing are likely the primary reasons for the observed phenomena.

Keywords Electropulsing · Machinability · GH4169 superalloy · Coupling of thermal and athermal effects

1 Introduction

GH4169 is a precipitation strengthened nickel-based superalloy. It is widely employed in the aerospace industry, in particular in the hot sections of gas turbine engines due to its excellent mechanical properties at elevated temperatures and good corrosion resistance [1–3]. Nickel-based superalloys are generally known to be one of the most difficult-to-cut materials because of their serious work hardening, high cutting force, affinity to react with the tool materials, and low thermal diffusivity [4–10]. These machining defects would lead to poor machined surface. Consequently, it is very important to find an appropriate method to improve the machinability of GH4169.

Nowadays, the researches on the improvement of the machinability of GH4169 are mainly focused on cutting tools [11–13], high-speed machining [10, 14], and external field assisted machining [15–19]. External field has long been widely used in materials processing such as laser field, ultrasonic field, and electric field. Anderson et al. [16] reported the benefit of laser-assisted machining (LAM) of Inconel 718, which was demonstrated by a 25% decrease in specific cutting energy, a 2–3-fold improvement in surface roughness and a 200–300% increase in ceramic tool life over conventional machining. Mitrofanov et al. [17] dealt with finite element modeling of ultrasonically assisted turning (UAT); they found that the finished surface was superior and the cutting process of Inconel 718 had an obvious decrease in cutting force and working temperatures with a high frequency of 20 kHz and amplitude of 10 μm.

Recently, electropulsing, as an instantaneous high energy input method, has been diffusely employed to assist the deformation and control the microstructure of metallic materials in the past 50 years [20–26]. Because of the coupling of thermal and athermal effects of electropulsing [27–29], the mobility of dislocations, atomic diffusion, and vacancy diffusion could be enhanced, which could lead to a better facilitation of plastic deformation. Electropulsing has the characteristics such as convenient, low-cost, and pollutant-free, which could make it ideal to assist the plastic deformation [30, 31]. Wang et al. [32] reported that electropulsing-assisted turning process (EP-TP) is an effective method to improve both the machinability and surface quality of AISI304 stainless steel. Baranov et al. [33] suggested that after electropulsing-assisted cutting

✉ G. Tang
tanggy@sz.tsinghua.edu.cn

[1] Advanced Materials Institute, Graduate School at Shenzhen, Tsinghua University, Shenzhen 518055, People's Republic of China

[2] School of Materials Science and Engineering, Tsinghua University, Beijing 100084, People's Republic of China

process, the friction force and processing time were decreased by 25–30 and 10–12%, respectively, compared with the traditional process. Our previous studies on electropulsing-assisted plastic deformation [34–38] also indicated that the plastic deformation and the quality of the machined surface could be improved markedly under the influence of electropulsing with proper parameters. However, there are few reports on the EP-TP of GH4169 superalloy. Therefore, the machinability, the micromorphology, and the microstructure of the machined surface during traditional dry turning process (TD-TP) and EP-TP were investigated in depth in this work.

2 Experimental procedures

The chemical composition of GH4169 superalloy is shown in Table 1. The cylindrical samples with the diameter of 21 mm and the length of 120 mm were prepared for the subsequent experiments. TD-TP and EP-TP were performed on a self-designed platform. The cutting speed was 26.4 m/min. The feed rate and the depth of cut were 0.2 mm/rev and 0.1 mm, respectively. YG6X tools were used for machining GH4169. The angle of tools in all cutting process remained unchanged. The rank angle was 6°. The clearance angle was 6°. The principal cutting edge angle and the tilt angle were 95° and 6°, respectively. The nose curvature radius was 0.2 mm. All of the experiments were done under dry cutting conditions.

The self-designed platform is shown in Fig. 1, which is based on a traditional lathe. The tailstock and the cutting tool are insulated with the lathe. The electropulsing generator designed by ourselves can supply pulse with a very sharp waveform. The peak current of pulse can reach up to 10,000 A. Because of the high energy and instantaneity of electropulsing, the Joule thermal effect is not obvious. Therefore, the athermal effects of electropulsing are the main focuses of this work. The current circuit is the positive of the generator → the positive graphite brush → the spindle chuck → the cylindrical sample → the lathe tailstock → the negative graphite brush → the negative of the generator.

The electropulsing parameters including frequency, RMS current density J_e, amplitude density J_m, and duration of electropulsing were obtained by a Hall Effect sensor connected to an oscilloscope. The electropulsing parameters used during TD-TP and EP-TP are listed in Table 2, and the width of pulse is about 90 μs. The main cutting force was calculated by the method which was reported by Liu [39]. The axial surface

Table 1 Chemical composition of GH4169 superalloy (wt%)

Element	Ni	Cr	Fe	Nb + Ta	Mo	Ti	Co	Al	Si
Content	51.55	19.62	Bal.	5.08	3.03	1.08	< 1.0	0.58	0.17

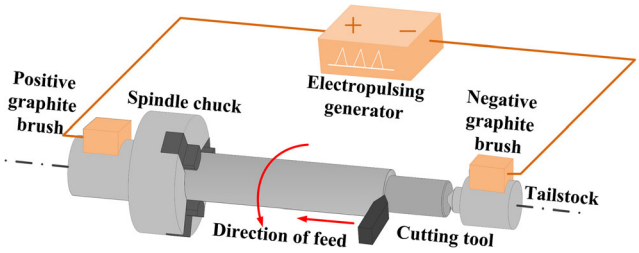

Fig. 1 The schematic diagram of TD-TP and EP-TP

roughness was measured by Surtronic S25 contact type surface roughness tester and Mitutoyo SJ-210 portable surface roughness tester. The microhardness was obtained by a HVS-1000B micro-Vickers hardness tester with a 100-g testing force and a 15-s load hold time. Meanwhile, each test of the axial surface roughness and the microhardness was performed at least five times and the average was taken. Surface temperature of the chips in the cutting area was measured using FLIR SC655 infrared thermal imager, and a K-type thermocouple was used to adjust the infrared emissivity of the specimens. KH-7700 digital microscope was used to observe the micromorphology of machined surface. Hitachi S4800 scanning electron microscope (SEM) was utilized to analyze cross-sectional microstructure and obtain electron backscatter diffraction (EBSD) maps.

3 Results and discussion

3.1 The main cutting force

The main cutting force is shown in Fig. 2. There is a downtrend in the main cutting force when electropulsing is applied.

Table 2 Electropulsing parameters used during TD-TP and EP-TP for GH4169 superalloy

Specimen no.	Frequency (Hz)	J_e (A mm^{-2})	J_m (A mm^{-2})
0	0	0	0
A1	300	0.34	2.87
A2	300	0.51	4.21
A3	300	0.64	4.92
A4	300	0.80	6.17
B1	400	0.34	2.87
B2	400	0.51	4.21
B3	400	0.64	4.92
B4	400	0.80	6.17
C1	500	0.34	2.87
C2	500	0.51	4.21
C3	500	0.64	4.92
C4	500	0.80	6.17

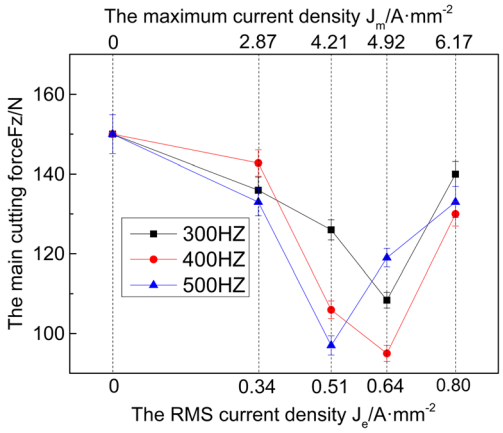

Fig. 2 The main cutting force of GH4169 superalloy

The main cutting force is about 150 N in TD-TP. When J_e is lower than 0.64 A mm^{-2}, the main cutting forces at different frequencies show a significant reduction with the increase of J_e. At the frequency of 400 Hz and the J_e of 0.64 A mm^{-2}, the main cutting force is optimal with the value of 95 N, which suggests a reduction of 36.7% compared with the TD-TP. However, with the further increase of J_e, the Joule thermal effect cannot be ignored due to the appearance of the yellowing surface. Thus, the cutting process is toilsome to be carried out and the main cutting force increases sharply. In addition, the frequency of electropulsing also has an obvious effect on the main cutting force under the same J_e. Tang et al. [38] reported that the electroplastic effect is most obvious at a certain frequency. With respect to GH4169, the optimum frequency is about 400 Hz under the given cutting parameters.

The maximum temperature in the turning process appears on the rake face, at which location is in contact with the chip, and it rises with the increase of J_e as shown in Fig. 3. Since there is some fluctuation of infrared emissivity due to the large range of the maximum temperature and a certain degree of surface oxidation, the maximum temperature on chip surface shown in Fig. 3 is not a strict absolute value. Nevertheless, the

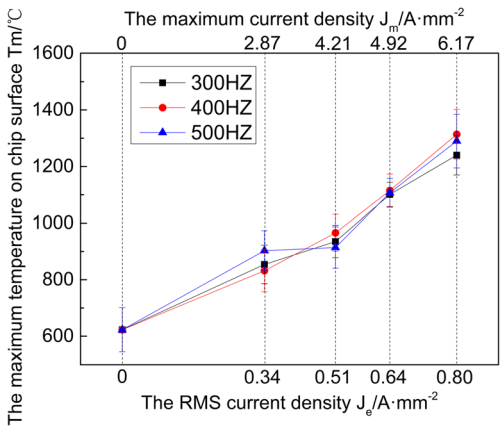

Fig. 3 The maximum temperature on chip surface of GH4169 specimens

machinability of GH4169 after TD-TP and EP-TP can be evaluated by the relative value of the maximum temperature. The maximum temperature is closely related to J_e but has little connection with the frequency of electropulsing. The ability of plastic deformation in the cutting area can be enhanced, and the work hardening can be weaken in a certain range of temperature rise [32]. When J_e is 0.80 A mm^{-2}, the maximum temperature is higher than 1200 °C and the machined surface displays a yellowing phenomenon. This is not conductive to a smooth cutting process and a high quality of machined surface of GH4169 superalloy.

3.2 The quality of machined surface

The axial surface roughness of GH4169 specimens after TD-TP and EP-TP is shown in Fig. 4. Compared with TD-TP specimen, the quality of machined surface of EP-TP specimens presents a dramatic enhancement as shown in Fig. 4a. For TD-TP specimen, the average axial surface roughness is Ra 4.47 μm, which corresponds to Fig. 4b. For EP-TP specimens, the axial surface roughness shows a significant decline with the increase of J_e in the range of less than 0.64 A mm^{-2}. At the lowest point, the axial surface roughness reaches the optimal value of Ra 1.14 μm at the frequency of 400 Hz as illustrated in Fig. 4c, which signifies a 74.5% decline compared with the TD-TP specimen. With the increasing of J_e, the rapid decrease in the surface roughness at the beginning is strongly dependent on the significant enhancement of plastic deformation, which is related to the reduced main cutting force and increased temperature in the cutting area. In addition, CR Green et al. [40] reported that electrically assisted manufacturing (EAM) could be employed to reduce or eliminate springback. With the decline of the springback, the surface finish could also be enhanced. When J_e is larger than 0.64 A mm^{-2}, the axial surface roughness begins to pick up, which signifies the deterioration of the machined surface.

The micromorphology of machined surface after TD-TP and EP-TP at 400 Hz is depicted in Fig. 5. During TD-TP, there exists a severe plastic shear deformation due to the serious work hardening in the cutting area on the surface of GH4169, resulting in apparent cutting edges and some broken edges between the cutting grooves, just as Fig. 5 (a-1), (a-2) shows. After electropulsing is introduced, the machined surface micromorphology shows a great improvement (Fig. 5 (b-1)) and the 3D micromorphology of EP-TP specimen at 0.34 A mm^{-2} (Fig. 5 (b-2)) exhibits a smoother surface than TD-TP (Fig. 5 (a-2)). The quality of machined surface can achieve a further enhancement with J_e increasing before 0.64 A mm^{-2}. As depicted in Fig. 5 (d-1), (d-2), the raised edges become flatted with the relatively evenly continuous edges among the cutting grooves. However, the enhancement in the surface quality is suppressed when J_e is higher than 0.64 A mm^{-2}, just as Fig. 5 (e-1), (e-2) shows. The evolution

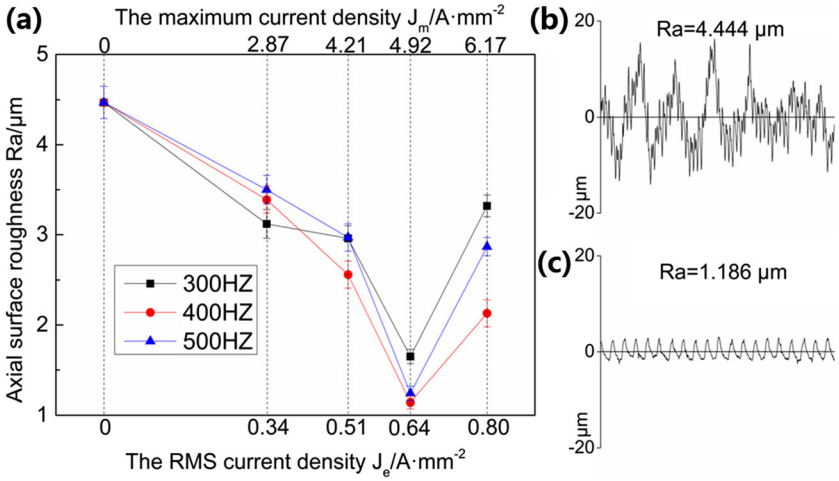

Fig. 4 Axial surface roughness of GH4169 specimens after TD-TP and EP-TP. **a** Surface roughness distribution curve. **b** TD-TP specimen. **c** EP-TP specimen at 400 Hz and 0.64 A mm^{-2}

of the micromorphology of machined surface shows that EP-TP can facilitate the plastic deformation ability to obtain a better surface quality than TD-TP.

3.3 The surface microhardness

Figure 6 shows the microhardness of the machined surface measured in the center of cutting grooves. The original microhardness of GH4169 sample is about 263 HV, which is expressed as a straight line in the bottom of Fig. 6. After TD-TP, the surface microhardness has a sharp increase and it can reach as high as 450 HV due to the serious work hardening during the cutting process. With the introduction of electropulsing, the resistance of shear deformation in the cutting area is reduced; thus, the plastic deformation is relatively easy to be carried out, and the work hardening can be weakened to some extent. Therefore, the surface microhardness has an evident decline, and it can reach the minimum value of 372 HV at the J_e of 0.64 A mm^{-2} and frequency of 300 Hz, which is

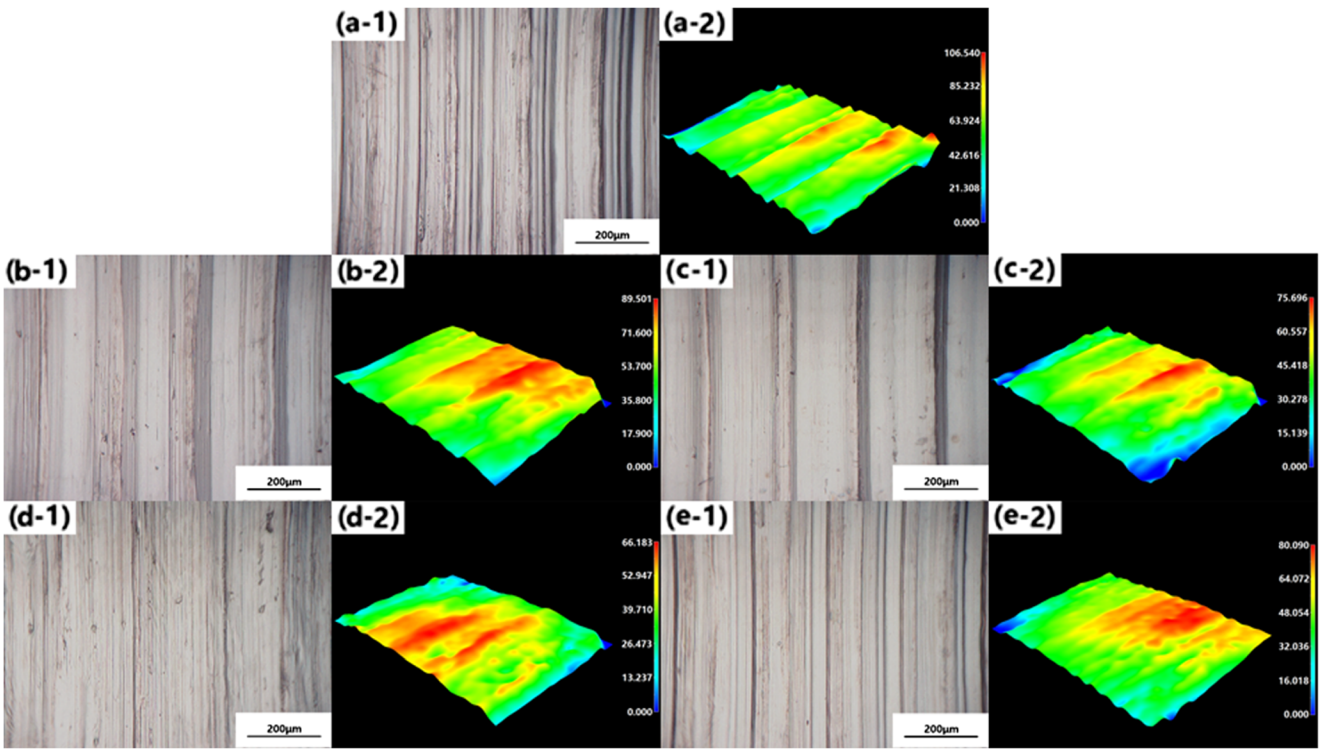

Fig. 5 Micromorphology of machined surface after TD-TP and EP-TP at 400 Hz: (a-1), (a-2) TD-TP specimen; (b-1), (b-2) EP-TP at 0.34 A mm^{-2}; (c-1), (c-2) EP-TP at 0.51 A mm^{-2}; (d-1), (d-2) EP-TP at 0.64 A mm^{-2}; (e-1), (e-2) EP-TP at 0.80 A mm^{-2}

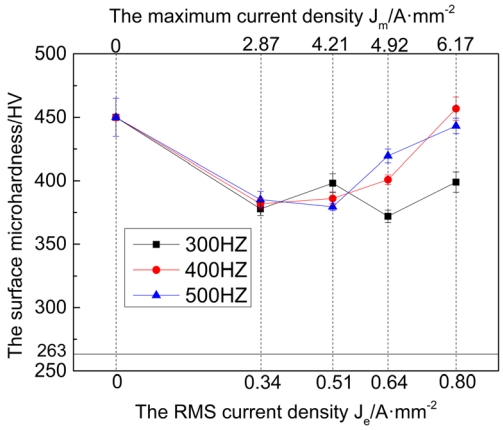

Fig. 6 The surface microhardness in the center of cutting grooves of GH4169 specimens

reduced by 17.3% compared with TD-TP specimen. However, when J_e is higher than 0.64 A mm^{-2}, the surface microhardness increases because of the surface oxidation, which is related to the Joule heat effect of electropulsing. Thus, the improvement of plastic deformation ability is partially offset, which has a bad influence on the machined surface quality just as Fig. 5 (e-1), (e-2) shows.

3.4 Influence of electropulsing on the microstructure of GH4169

Figure 7 demonstrates the microstructure of GH4169 specimens. The surface microstructure is shown in Fig. 7 (a-1), (b-1), and the EBSD maps of the corresponding microstructure in strengthened layer are depicted in Fig. 7 (a-3), (b-3). Since the serious work hardening during TD-TP, the ability of plastic deformation is easily restricted, resulting in a thin deformation layer about 2–3 μm on the machined surface. When the electropulsing with the frequency of 400 Hz and the J_e of 0.64 A mm^{-2} is applied, the ability of plastic deformation is reinforced and the plastic flow is more severe than what Fig. 7 (a-1) shows. Therefore, further plastic deformation on surface is enhanced and the depth of plastic deformation is deepened. The deformation layer after EP-TP (at the frequency of 400 Hz and the J_e of 0.64 A mm^{-2}) is about 7–8 μm, almost two to three times that of TD-TP. Furthermore, the sub-grain boundaries shown in Fig. 7 (a-3), (b-3) are defined for misorientations between 2° and 10°, while the grain boundaries are defined upper than 10°. The sub-grain boundaries are increased in EP-TP specimen (Fig. 7 (a-3)) compared with that in TD-TP specimen (Fig. 7 (a-3)). Therefore, the formation of substructure is enhanced under the effects of electropulsing, indicating the facilitation of plastic deformation of GH4169 superalloy during the turning process. In addition, the internal microstructure is depicted in Fig. 7 (a-2), (b-2). There is no obvious change in the center microstructure of specimens.

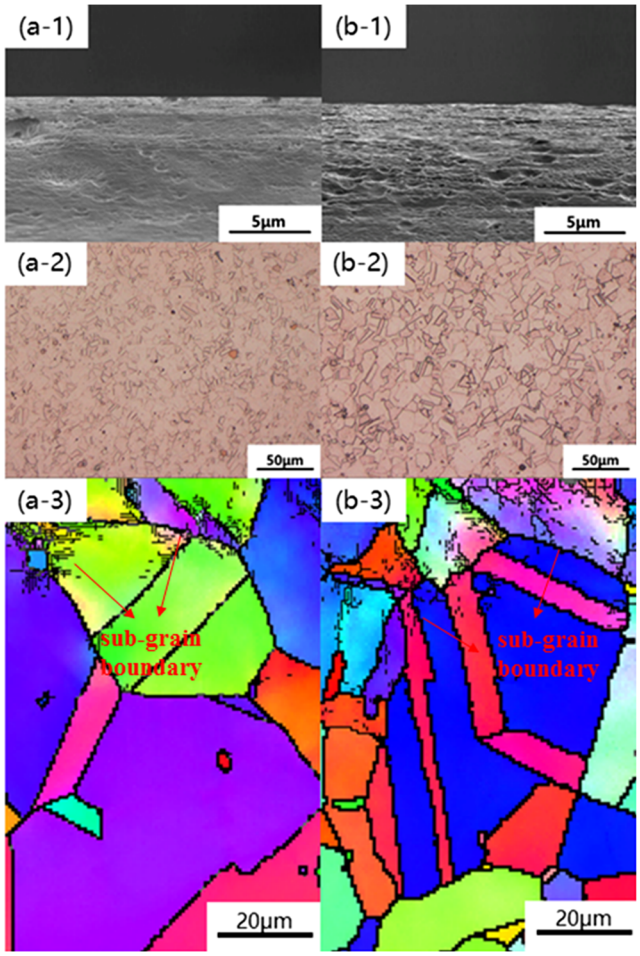

Fig. 7 The microstructure and EBSD maps of GH4169 superalloy: (a-1), (a-2), (a-3) TD-TP specimen; (b-1), (b-2), (b-3) EP-TP specimen at the frequency of 400 HZ and the J_e of 0.64 A mm^{-2}

Thus, the electropulsing introduced in the turning process mainly acts on the surface of GH4169 specimens and has little effect on the internal of materials.

4 Discussion

The significant improvement in machinability of GH4169 during EP-TP at proper electropulsing parameters can be mainly attributed to the enhancement of plastic deformation ability induced by electropulsing. Meanwhile, the micromechanism of plastic deformation is the creation and movement of dislocations in materials. In TD-TP, the increase in dislocation density and the interaction between dislocations and defects in shear deformation result in tangled dislocations; then, the mobility of dislocations is restricted and eventually work hardening occurs. Thus, further plastic deformation has reduced likelihood to take place. Extensive studies [20, 21, 41] were performed along the influence of electropulsing on the metals, but

there is still no agreement to explain the phenomenon mentioned above. These previous theories are generally agreed that the thermal (Joule effect) and athermal effects play an important role in accelerating the movement of dislocations and overcoming the resistance from obstacles, thereby resulting in a decrease in resistance and an increase in plasticity.

The Joule effect was found to be the most important side effect during EP-TP. It can inevitably generate heat due to electrical resistance. The temperature rise is [42]

$$\Delta T = \frac{\rho J^2 t_p}{c_p d} \tag{1}$$

where ρ is the total resistivity, J is the current density of electropulsing, t_p is the electropulsing duration, c_p is the specific heat, and d is the density of sample. Equation (1) indicates that the temperature rise is proportional to the square of the current density. A certain temperature can supply activation energy to facilitate dislocation mobility and atom diffusion due to their conquered migration energy barriers [43]. Therefore, with the application of electropulsing, GH4169 specimens could be softened and then the turning process could be easier to be proceeded. However, due to the short duration of electropulsing and the nondirection of heat transfer [35], Joule effect plays an assistant role in improving the mechanical properties of GH4169 superalloy.

Compared with the thermal effect, the athermal effect is more important to increase the mobility of dislocations. When the electropulsing is applied, the drift electrons could exert mechanical stress on dislocations [20] and then the mobility of dislocations could be enhanced. This mechanical stress is called electron wind force. Worked by the current, the electron wind force F_e on per unit length dislocation by the drift electrons in the same direction is [38]

$$F_e = \frac{b}{4}\left(\frac{V_e}{V_d} - 1\right)\frac{V_d \partial n_0}{V \partial \mu}\Delta^2 \tag{2}$$

where b is Burgers vector, V_e is the drift velocity of the electrons, V_d is the speed of dislocations, V is the speed of the electrons in the Fermi plane, n_0 is the density of the free carrier, μ is the chemical potential, and $\triangle$ is the deformation potential constant. According to Eq. (2), when $V_e > V_d$, the force of free electrons is normal. That is, the movement of the dislocations is accelerated. The drift electrons on dislocations have stronger forces corresponding to higher current density, which leads to the acceleration of dislocations.

In addition, the concentration of vacancy is increased under the effect of electropulsing [44]. During the turning process, some defects are inevitably produced in GH4169 samples. Since the electrical resistivity is sensitive to the microstructural details, an inhomogeneous physical field could be formed, and the electrical resistivity is larger in the area with defects than that in the area without defects [45]. This could lead to a different temperature rise in metal when the electropulsing is introduced in the turning process. Since the thermal expansion lags behind the temperature rise [46], a transient high thermal compressive stress comes into being during the expansion running after temperature rise. Under this stress effect, the concentration of vacancy is increased. Therefore, the dislocation reaction and dislocation mobility could be promoted, which can eventually facilitate the rearrangement and disappear of dislocations.

Accordingly, all of the mechanisms mentioned above can promote the mobility of dislocations and ability of plastic flow, which could lead to the decrease of the internal friction during the plastic deformation process. Apart from that, with the application electropulsing, the lubricating property between samples and cutting tools could be enhanced. On one hand, the particulate on the surface of samples of which location is in contact with cutting tools could be forced to vibrate by the action of electropulsing. On the other hand, the surface work function could be changed by the external electric field [38]. Since the surface hardness and surface energy, related to the friction force, are positively correlated with the surface work function [47], the friction factor between to-be-cut material and cutting tools could be reduced by the electropulsing with the proper frequency and current density. Thus, this could facilitate an even cutting process and a smooth machined surface in EP-TP with proper electropulsing parameters.

In this research, the frequency of electropulsing also has an important effect on the cutting process. Tang et al. [-38]introduced the theory of quantum mechanics wave into the study of the influence of electropulsing on the plasticity of metallic materials. The atoms in the metal are periodically arranged; thus, the corresponding potential energy and electron density also have a periodic distribution. Therefore, the periodic arrangement of this metal atoms can be regarded as a matter wave and it can be described by the superposition of harmonics based on Fourier decomposition [48]. Therefore, when the frequency of electropulsing introduced in this research is close to the frequency of the matter wave in metal, it will lead to a resonance effect, resulting in a strong electroplastic effect. In addition, Postnikov et al. [48] indicated that the formation of internal defects begins with the distortion of its electronic structure. With the apparent distortion of electron density distribution in metals, the plastic deformation is easy to occur. Therefore, when the electropulsing with the certain frequency and current density is applied in the turning process, there will be a resonance effect between electropulsing and to-be-cut material, and then the electronic structure of materials has an instantaneous serious distortion. Thereby, the ability of plastic deformation could be improved noticeably.

To sum up, EP-TP is a nonequilibrium process [45]. The effect of electropulsing used in this study is 2-fold. On one

hand, the Joule effect can generate a slightly high surface equilibrium temperature on the specimen, which plays an assistant role in facilitating dislocation mobility. On the other hand, due to the interaction between electropulsing and material itself, athermal effects such as electron wind force, transient thermal compressive stress, and resonance effect play predominant roles in accelerating the movement of dislocations and overcoming the resistance from obstacles. Therefore, under this coupling of thermal and athermal effects by electropulsing, the plastic deformation is enhanced and the cutting process is easily to be carried out, which can eventually improve the machinability and surface quality of GH4169 superalloy.

5 Conclusion

In the present work, electropulsing is introduced in the turning process of GH4169 superalloy. The machinability, surface quality, and surface microstructure during TD-TP and EP-TP are carefully characterized. In EP-TP at the frequency of 400 Hz and the J_e of 0.64 A mm^{-2}, the main cutting force, the axial surface roughness, and the surface microhardness are reduced by 36.7, 74.5, and 17.3% compared with TD-TP, respectively. In addition, the depth of the surface deformation layer after EP-TP can be two to three times that of TD-TP and the sub-grain boundaries are increased under the influence of electropulsing. The microstructure evolution of strengthened layer signifies the enhanced ability of the plastic deformation in EP-TP. Therefore, a stable cutting process and a smooth machined surface can be guaranteed under the effect of electropulsing with appropriate electropulsing parameters.

Funding information The authors wish to acknowledge the financial support from the Engineering Laboratory Project of Shenzhen Development and Reform Commission (No. 2015-1033) and the Shenzhen Science and Technology supporting Plan Project (No. GJHS20160331183313435).

References

1. Lv P, Sun X, Cai J, Zhang C, Liu X, Guan Q (2017) Microstructure and high temperature oxidation resistance of nickel based alloy GH4169 irradiated by high current pulsed electron beam. Surf Coat Technol 309:401–409. https://doi.org/10.1016/j.surfcoat.2016.11.041
2. Yao CF, Jin QC, Huang XC, DX W, Ren JX, Zhang DH (2013) Research on surface integrity of grinding Inconel718. Int J Adv Manuf Technol 65(5–8):1019–1030. https://doi.org/10.1007/s00170-012-4236-7
3. Kuppan P, Rajadurai A, Narayanan S (2008) Influence of EDM process parameters in deep hole drilling of Inconel 718. Int J Adv Manuf Technol 38(1–2):74–84. https://doi.org/10.1007/s00170-007-1084-y
4. Sharman A, Dewes RC, Aspinwall DK (2001) Tool life when high speed ball nose end milling Inconel 718. J Mater Process Technol 118(1-3):29–35. https://doi.org/10.1016/S0924-0136(01)00855-X
5. Ezugwu EO, Wang ZM, Machado AR (1999) The machinability of nickel-based alloys. J Mater Process Technol 86(1-3):1–16. https://doi.org/10.1016/S0924-0136(98)00314-8
6. Li L, He N, Wang M, Wang ZG (2002) High speed cutting of Inconel 718 with coated carbide and ceramic inserts. J Mater Process Technol 129(1-3):127–130. https://doi.org/10.1016/S0924-0136(02)00590-3
7. Jawaid A, Koksal S, Sharif S (2001) Cutting performance and wear characteristics of PVD coated and uncoated carbide tools in face milling Inconel 718 aerospace alloy. J Mater Process Technol 116(1):2–9. https://doi.org/10.1016/S0924-0136(01)00850-0
8. Rahman M, Seah WKH, Teo TT (1997) The machinability of Inconel 718. J Mater Process Technol 63(1-3):199–204. https://doi.org/10.1016/S0924-0136(96)02624-6
9. Dudzinski D, Devillez A, Moufki A, Larrouquère D, Zerrouki V, Vigneau J (2004) A review of developments towards dry and high speed machining of Inconel 718 alloy. Int J Mach Tool Manu 44(4):439–456. https://doi.org/10.1016/S0890-6955(03)00159-7
10. Thakur DG, Ramamoorthy B, Vijayaraghavan L (2009) Machinability investigation of Inconel 718 in high-speed turning. Int J Adv Manuf Technol 45(5–6):421–429. https://doi.org/10.1007/s00170-009-1987-x
11. Altin A, Nalbant M, Taskesen A (2007) The effects of cutting speed on tool wear and tool life when machining Inconel 718 with ceramic tools. Mater Des 28(9):2518–2522. https://doi.org/10.1016/j.matdes.2006.09.004
12. Bhatt A, Attia H, Vargas R, Thomson V (2010) Wear mechanisms of WC coated and uncoated tools in finish turning of Inconel 718. Tribol Int 43(5–6):1113–1121. https://doi.org/10.1016/j.triboint.2009.12.053
13. Zhou J, Avdovic P, Ståhl JE (2012) Study of surface quality in high speed turning of Inconel 718 with uncoated and coated CBN tools. Int J Adv Manuf Technol 58(1–4):141–151. https://doi.org/10.1007/s00170-011-3374-7
14. Amini S, Fatemi MH, Atefi R (2014) High speed turning of Inconel 718 using ceramic and carbide cutting tools. Arab J Sci Eng 39(3):2323–2330. https://doi.org/10.1007/s13369-013-0776-x
15. Hsu CY, Lin YY, Lee WS, Lo SP (2008) Machining characteristics of Inconel 718 using ultrasonic and high temperature-aided cutting. J Mater Process Technol 198(1–3):359–365. https://doi.org/10.1016/j.jmatprotec.2007.07.015
16. Anderson M, Patwa R, Shin YC (2006) Laser-assisted machining of Inconel 718 with an economic analysis. Int J Mach Tools Manuf 46(14):1879–1891. https://doi.org/10.1016/j.ijmachtools.2005.11.005
17. Mitrofanov AV, Babitsky VI, Silberschmidt VV (2004) Finite element analysis of ultrasonically assisted turning of Inconel 718. J Mater Process Technol 153-154:233–239. https://doi.org/10.1016/j.jmatprotec.2004.04.299
18. Li S, Wu Y, Nomura M (2016) Effect of grinding wheel ultrasonic vibration on chip formation in surface grinding of Inconel 718. Int J Adv Manuf Technol 86(1–4):1113–1125. https://doi.org/10.1007/s00170-015-8149-0
19. ZW D, Chen Y, Zhou K, Li C (2015) Research on the electrolytic-magnetic abrasive finishing of nickel-based superalloy GH4169. Int J Adv Manuf Technol 81(5–8):897–903
20. Sprecher AF, Mannan SL, Conrad H (1986) Overview no. 49 : on the mechanisms for the electroplastic effect in metals. Acta Metall 34(7):1145–1162. https://doi.org/10.1016/0001-6160(86)90001-5
21. Troitskii OA (1985) Pressure shaping by the application of a high energy. Mater Sci Eng 75(1–2):37–50
22. Jiang Y, Tang G, Shek C, Zhu Y, Guan L, Wang S, Xu Z (2009) Improved ductility of aged Mg-9Al-1Zn alloy strip by

electropulsing treatment. J Mater Res 24(5):1810–1814. https://doi.org/10.1557/jmr.2009.0197
23. Liu T, Li X, Tang G, Song G (2016) Effect of ultrasonic impact treatment assisted with high energy electropulsing on microstructure of D36 carbon steel. J Mater Res 31(24):3956-3967
24. Qin RS, Rahnama A, WJ L, Zhang XF, Elliottbowman B (2014) Electropulsed steels. Mater Sci Technol 30(9):1040–1044. https://doi.org/10.1179/1743284714Y.0000000533
25. Wu HB, To S (2016) Effects of electropulsing treatment on material properties and ultra-precision machining of titanium alloy. Int J Adv Manuf Technol 82(9–12):2029–2036. https://doi.org/10.1007/s00170-015-7379-5
26. Lou Y, Wu H (2017) Improving machinability of titanium alloy by electro-pulsing treatment in ultra-precision machining. Int J Adv Manuf Technol 93(5-8):2299-2304
27. Jiang Y, Tang G, Guan L, Wang S, Xu Z, Shek C, Zhu Y (2008) Effect of electropulsing treatment on solid solution behavior of an aged Mg alloy AZ61 strip. J Mater Res 23(10):2685–2691. https://doi.org/10.1557/JMR.2008.0328
28. Samuel EI, Bhowmik A, Qin R (2010) Accelerated spheroidization induced by high intensity electric pulse in a severely deformed eutectoid steel. J Mater Res 25(6):1020–1024. https://doi.org/10.1557/JMR.2010.0140
29. Jiang Y, Tang G, Shek C, Zhu Y, Xu Z (2009) On the thermodynamics and kinetics of electropulsing induced dissolution of β-Mg17Al12 phase in an aged Mg–9Al–1Zn alloy. Acta Mater 57(16):4797–4808. https://doi.org/10.1016/j.actamat.2009.06.044
30. Ma B, Zhao Y, Ma J, Guo H, Yang Q (2013) Formation of local nanocrystalline structure in a boron steel induced by electropulsing. J Alloys Compd 549:77–81. https://doi.org/10.1016/j.jallcom.2012.09.047
31. Hameed S, Rojas HAG, Egea AJS, Alberro AN (2016) Electroplastic cutting influence on power consumption during drilling process. Int J Adv Manuf Technol 87(5-8):1835-1841
32. Wang H, Chen L, Liu D, Song G, Tang G (2015) Study on electropulsing assisted turning process for AISI 304 stainless steel. Mater Sci Technol 31(13):1564–1571. https://doi.org/10.1179/1743284715y.0000000034
33. Baranov SA, Staschenko VI, Sukhov AV, Troitskiy OA, Tyapkin AV (2011) Electroplastic metal cutting. Russ Electr Eng 82(9):477–479. https://doi.org/10.3103/s1068371211090033
34. Li X, Li X, Zhu J, Ye X, Tang G (2016) Microstructure and texture evolution of cold-rolled Mg-3Al-1Zn alloy by electropulse treatment stimulating recrystallization. Scr Mater 112:23–27. https://doi.org/10.1016/j.scriptamat.2015.09.001
35. Ye Y, Kuang J, Kure-Chu S-Z, Song G, Sun Z, Tang G (2016) Improvement of microstructure and surface behaviors of welded S50C steel components under electropulsing assisted ultrasonic surface modification. J Mater Res 31(14):2125–2135. https://doi.org/10.1557/jmr.2016.127
36. Wang H, Song G, Tang G (2016) Effect of electropulsing on surface mechanical properties and microstructure of AISI 304 stainless steel during ultrasonic surface rolling process. Mater Sci Eng A 662:456–467. https://doi.org/10.1016/j.msea.2016.03.097
37. Kuang J, Li X, Ye X, Tang J, Liu H, Wang J, Tang G (2015) Microstructure and texture evolution of magnesium alloys during electropulse treatment. Metall Mater Trans A 46(4):1789–1804. https://doi.org/10.1007/s11661-014-2735-x
38. Tang G, Zhang J, Zheng M, Zhang J, Fang W, Li Q (2000) Experimental study of electroplastic effect on stainless steel wire 304L. Mater Sci Eng A 281(1–2):263–267. https://doi.org/10.1016/S0921-5093(99)00708-X
39. Liu F, Xu Z (1988) A new method measuring and calculationg the energy efficiency, cutting torque and cutting force. Manuf Technol Mach Tool 31(6):14–15
40. Green CR, McNeal TA, Roth JT (2009) Springback elimination for Al-6111 alloys using electrically-assisted manufacturing (EAM). Trans North Am Manuf Res Inst SME 37:403–410
41. Conrad H (2000) Electroplasticity in metals and ceramics. Mater Sci Eng: Struct Mater Prop Microstruct Process 287(2):276–287. https://doi.org/10.1016/S0921-5093(00)00786-3
42. Okazaki K, Kagawa M, Conrad H (1980) An evaluation of the contributions of skin, pinch and heating effects to the electroplastic effect in titanium. Mater Sci Eng 45(2):109–116
43. Wang H, Song G, Tang G (2016) Evolution of surface mechanical properties and microstructure of Ti 6Al 4V alloy induced by electropulsing-assisted ultrasonic surface rolling process. J Alloys Compd 681:146–156. https://doi.org/10.1016/j.jallcom.2016.04.067
44. Xu Z, Tang G, Tian S, He J (2006) Research on the engineering application of multiple pulses treatment for recrystallization of fine copper wire. Mater Sci EngA 424(1):300–306. https://doi.org/10.1016/j.msea.2006.03.012
45. Zhang W, Sui ML, Zhou YZ, Li DX (2003) Evolution of microstructures in materials induced by electropulsing. Micron 34(3–5):189–198. https://doi.org/10.1016/S0968-4328(03)00025-8
46. Tang DW, Zhou BL, Cao H, He GH (1991) Dynamic thermal expansion under transient laser-pulse heating. Appl Phys Lett 59(24):3113–3114. https://doi.org/10.1063/1.105755
47. Rabinowicz E (1965) Friction and wear of materials. Wiley, New York, pp 10-30
48. Postnikov SN (1978) Electrophysical and electrochemical phenomena in friction, cutting, and lubrication. Van Nostrand Reinhold, New York